TISSUE ENGINEERING: Part A
Volume 16, Number 4, 2010

DOI: 10.1089/ten.tea.2009.0480

Functional Properties of Cell-Seeded Three-Dimensionally Woven Poly(ε-Caprolactone) Scaffolds for Cartilage Tissue Engineering

Franklin T. Moutos, Ph.D., and Farshid Guilak, Ph.D.

Articular cartilage possesses complex mechanical properties that provide healthy joints the ability to bear repeated loads and maintain smooth articulating surfaces over an entire lifetime. In this study, we utilized a fiber-reinforced composite scaffold designed to mimic the anisotropic, nonlinear, and viscoelastic biomechanical characteristics of native cartilage as the basis for developing functional tissue-engineered constructs. Three-dimensionally woven poly(ε-caprolactone) (PCL) scaffolds were encapsulated with a fibrin hydrogel, seeded with human adipose-derived stem cells, and cultured for 28 days in chondrogenic culture conditions. Biomechanical testing showed that PCL-based constructs exhibited baseline compressive and shear properties similar to those of native cartilage and maintained these properties throughout the culture period, while supporting the synthesis of a collagen-rich extracellular matrix. Further, constructs displayed an equilibrium coefficient of friction similar to that of native articular cartilage ($\mu_{eq} \sim 0.1–0.3$) over the prescribed culture period. Our findings show that three-dimensionally woven PCL–fibrin composite scaffolds can be produced with cartilage-like mechanical properties, and that these engineered properties can be maintained in culture while seeded stem cells regenerate a new, functional tissue construct.

Introduction

Articular cartilage is the load-bearing, wear-resistant surface that lines the ends of the long bones in diarthrodial joints. Under normal circumstances, this tissue permits a lifetime of normal musculoskeletal function by minimizing friction, distributing loads, and dissipating energy imparted on joints through daily activities. However, due to its avascularity and low biosynthetic activity, the tissue has a limited capacity to self-repair.[1] As a result, diseased or damaged cartilage degenerates progressively, ultimately leading to chronic pain and disability. Although current treatment options for full-thickness lesions such as microfracture and autologous chondrocyte transplantation have yielded encouraging clinical success, they can lead to the formation of biomechanically inferior fibrous tissue and are not necessarily suitable for large defects or joint resurfacing.[1–5]

In this regard, there has been growing interest in developing new tissue engineering strategies that seek to restore the biomechanical function of damaged musculoskeletal tissues. In general, these tissues are subjected to complex loading patterns that require tissue architectures with preferentially aligned fiber ultrastructures. Applying the principles of functional tissue engineering,[6,7] researchers have designed new composite scaffolds that incorporate organized reinforcing fibers and textile structures for the regeneration of cardiac tissue,[8] bone,[9–11] ligament,[12–14] meniscus,[15,16] and cartilage.[17–20] Focused specifically on recapitulating the complex biomechanical properties of articular cartilage, we have developed a three-dimensionally (3D) woven composite scaffold using biomaterials known to support chondrogenesis.[21,22] The basis of this design was a microscale 3D weaving technique that arranged multiple layers of load-bearing polyglycolic acid (PGA) fibers in three orthogonal directions. This woven fabric was then infiltrated with a cell-supporting hydrogel to form a composite construct with cartilage-like properties along each of its planes of symmetry. However, *in vitro* studies showed that chondrocyte-loaded constructs did not maintain their initial biomimetic properties over a 28-day culture period due to rapid fiber degradation and a lack of cell-mediated matrix accumulation.[23] Thus, the goal of this study was to improve the long-term functionality of the constructs by using an alternative fiber for weaving the 3D scaffolds, and to accelerate tissue synthesis by seeding with more metabolically active chondrogenic progenitor cells.

To this end, we used poly(ε-caprolactone) (PCL) fibers to weave a new reinforcing scaffold, which was seeded with cells suspended in a fibrin matrix to create a composite

Department of Surgery, Duke University Medical Center, Durham, North Carolina.

construct that mimics the functional properties of cartilage. Although autologous primary chondrocytes have been used extensively in cartilage tissue engineering applications, there are several limitations to this approach, including the lack of adequate healthy autologous tissue, the potential disease state of the harvested cells, the potential for initiating osteoarthritic changes in the joint through the harvesting process, and the difficulty in maintaining the chondrocytic phenotype during *ex vivo* expansion.[24–27] Thus, there remains a great need for identifying additional cell sources for use in cartilage tissue engineering. In this respect, we investigated the use of adult human adipose-derived stem cells (ASCs), an abundant and easily accessible population of multipotent progenitor cells that can be isolated from liposuction waste and have been previously investigated for use in cartilage tissue engineering.[2,28,29] Chondrogenic differentiation of ASCs has been shown to be induced using exogenously delivered growth factors,[30,31] genetic overexpression,[32] or biomaterial scaffolds.[33] Fibrin, a biopolymer comprised of fibrinogen monomer units, is derived from blood components and can act as a pro-chondrogenic scaffold for tissue engineering applications.[34–38] Like most hydrogels, fibrin has poor mechanical properties and has been combined with biomaterials such as polyurethane,[34] β-tricalciumphosphate,[39] polytetrafluroethylene,[40] and PCL[41] to form composite scaffolds with improved load-bearing function. PCL is a slowly degrading aliphatic polyester that has been shown to remain *in vivo* for up to 3 years.[42] This biomaterial has been approved for implantation by the Food and Drug Administration,[42,43] and exhibits good manufacturing characteristics and has been used extensively to produce scaffolds using a variety of manufacturing methods, including electrospinning,[16,44] fused deposition modeling,[45–47] and traditional textile processes.[41,48]

The overall objective of this study was to evaluate the functional biomechanical properties and chondrogenic potential of a PCL–fibrin composite scaffold over an extended *in vitro* culture period. Using a 3D weaving process, scaffolds capable of mimicking the complex multiphasic behavior and material properties of native articular cartilage immediately after manufacture were produced. We hypothesized that the combination of a load-bearing PCL structure encapsulated with human ASC-seeded fibrin hydrogel would allow for the rapid restoration and long-term maintenance of functional construct properties, while simultaneously supporting chondrogenic induction and extracellular matrix (ECM) synthesis.

Materials and Methods

Scaffold preparation

The 3D textile scaffold utilized in this study was produced using a custom-built miniature weaving loom as described previously.[21] Briefly, 156-μm-diameter multifilament PCL yarns (EMS-Griltech, Domat, Switzerland) were assembled into a multilayer fabric structure consisting of two perpendicularly oriented sets of in-plane fibers; five layers were aligned in the warp (x-direction) and six layers were aligned in the weft (y-direction) (Fig. 1). These 11 layers were interlocked with a third set of fibers (z-direction) that were passed vertically through the layers following a continuous, repeated path (Fig. 1B). Measuring 1.4 mm in thickness, the resulting structure contained a network of rectangular, interconnected pores with dimensions of approximately 330×260×100 μm and a final void fraction of approximately 60%. After weaving, the PCL fabric was immersed in a 4 M NaOH bath overnight to clean the fibers and increase their surface hydrophilicity.[49,50] It was then washed repeatedly with deionized water and dried at room temperature for 24 h. The cleaned fabric was sterilized by soaking in 70% ethanol overnight followed by UV exposure for 30 min per side. It was then placed in a sterile phosphate-buffered saline (PBS) bath overnight, washed three times (5 min each) in fresh PBS, and incubated in Dulbecco's modified Eagle's medium (DMEM; Gibco, Grand Island, NY) at 37°C for 4 h before cell seeding.

Composite scaffolds were formed using a vacuum-assisted molding technique to infuse the porous PCL structure with fibrin gel. Specifically, a 4×2 cm strip of fabric was placed in an air-tight vacuum pouch constructed on a rigid surface with injection and exhaust ports at opposing ends. With the injection port initially closed, vacuum was applied to the exhaust port to remove all the air from inside the pouch. The resulting negative pressure caused the bag to pull down tightly on the fabric and evacuate the material without collapsing its internal pore structure. Although maintaining the negative pressure, 1 mL of noncrosslinked fibrinogen

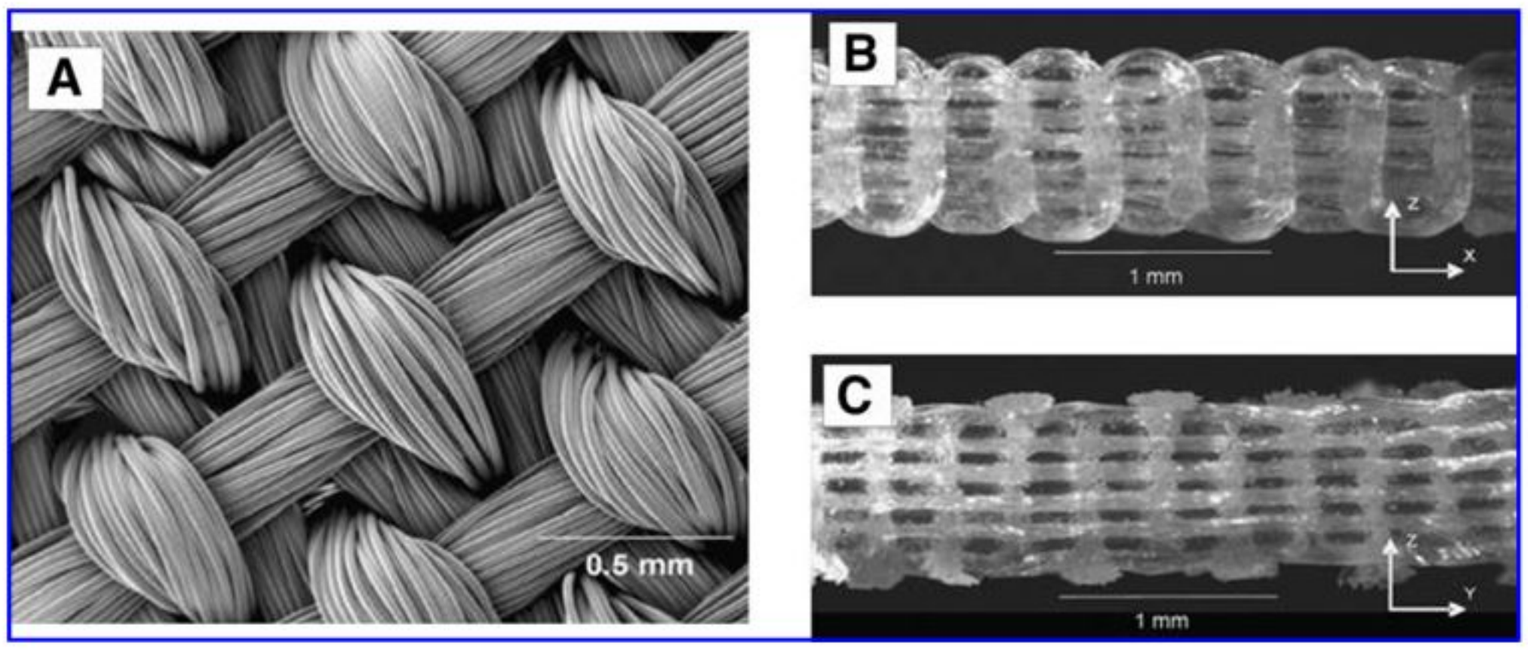

FIG. 1. Fiber architecture of a three-dimensionally orthogonally woven poly(ε-caprolactone) (PCL) structure. Three-dimensional structures were woven by interlocking multiple layers of two perpendicularly oriented sets of in-plane fibers (x- or warp direction, and y- or weft direction) with a third set of fibers in the z-direction. (**A**) Surface view of the X–Y plane (standard error of the mean [SEM]), (**B**) cross-sectional view of the X–Z plane, and (**C**) cross-sectional view of the Y–Z plane.

solution (100–130 mg/mL, Tisseel™; Baxter Biosurgery, Westlake Village, CA) was delivered into the pouch via the injection port. The pressure differential forced the solution through the length of the fabric in a controlled and even flow. Once the flow front reached the end of the fabric and complete wet-out was achieved, the vacuum was removed by closing off the exhaust port. The bag was then opened and the infiltrated fabric was bathed in thrombin solution (Tisseel; Baxter Biosurgery) for 5 min to crosslink the fibrin hydrogel. A biopsy punch was then used to cut individual 3-mm-diameter samples from the crosslinked composite.

In vitro *culture of constructs*

Human ASCs from the subcutaneous fat of seven different nonsmoking, nondiabetic female donors (ages 27–51 and body mass index 22.5–28.2) were obtained from liposuction waste (Zen-Bio, Durham, NC) and pooled after an initial passage used to test growth kinetics. The cells were plated on 225 cm^2 culture flasks (Corning, Corning, NY) at an initial density of 8000 cells/cm^2 and cultured at 37°C at 5% CO_2 in expansion medium consisting of DMEM–F12 (Cambrex Bio Science, Walkersville, MD), 10% fetal bovine serum (FBS; Atlas Biologicals, Ft. Collins, CO), 1% penicillin–streptomycin–Fungizone (Gibco), 0.25 ng/mL TGF-β1 (R&D Systems, Minneapolis, MN), 5 ng/mL epidermal growth factor (Roche Diagnostics, Indianapolis, IN), and 1 ng/mL basic fibroblast growth factor (Roche Diagnostics). Expansion medium was replaced every 2–3 days as needed until cells became 90% confluent, at which time they were trypsinized (0.05% trypsin–ethylenediaminetetraacetic acid; Gibco), resuspended in DMEM–F12 plus 10% FBS, counted with a hemacytometer, and replated. Cell viability was assessed using a trypan blue exclusion assay. All cells were passaged to P4 before being seeded onto scaffolds using the vacuum infusion technique described above. Cell-loaded PCL–fibrin composite constructs were formed by resuspending ASCs in the noncrosslinked fibrinogen solution at a concentration of 10 million cells/mL before vacuum infusion. For PCL-only constructs, ASCs were resuspended in DMEM (10 million cells/mL) and infused into the scaffold using the same technique. All constructs were cultured in 24-well low-attachment plates (Corning) in 0.5 mL of culture medium per well consisting of DMEM–high glucose (Gibco), 10% FBS (Atlas Biologicals), 37.5 μg/mL ascorbic-2-phosphate (Sigma-Aldrich, St. Louis, MO), 1% insulin, transferrin, selenous acid (ITS) + premix (Collaborative Biomedical–Becton-Dickinson, Bedford, MA), and 1% penicillin–streptomycin (Gibco). The media were completely changed every 2 days. Scaffolds were analyzed at 0-, 14-, and 28-day time points to assess chondrogenic development.

Evaluation of mechanical properties

Compressive (confined and unconfined configurations), shear, and frictional mechanical tests were performed on all samples ($n = 4$ per group) at days 0, 14, and 28 of culture. Tensile testing was only performed at baseline due to the size of the samples.

Compression testing

A confined-compression configuration was used to perform creep experiments on the engineered constructs using an ELF 3200 Series precision controlled materials testing system (Bose, Minnetonka, MN). The 3-mm-diameter cylindrical test specimens were placed in a confining chamber and compressive loads were applied using a solid piston against a rigid porous platen (porosity = 50%; pore size = 50–100 μm). After equilibration of a 10-gf tare load, a step compressive load of 30 grams-force (gf) was applied to the sample and allowed to equilibrate for 3600 s. The compressive aggregate modulus (H_A) and apparent hydraulic permeability (k) were determined numerically by matching the solution for axial strain (ε_z) to the experimental data for all creep tests using a two-parameter, nonlinear least-squares regression procedure.[51,52] For unconfined compression, strains of $\varepsilon = 0.04$, 0.08, 0.12, and 0.16 were applied to the specimens after equilibration of a 4-gf tare load. Strain steps were held constant for 900 s, allowing the scaffolds to relax to equilibrium. Young's modulus was determined by performing linear regression on the resulting equilibrium stress–strain plot.

Shear testing

Dynamic frequency sweep shear tests were performed using an ARES Rheometrics System (Rheometric Scientific, Piscataway, NJ). Samples were tested between two rigid porous platens in a PBS bath at room temperature. A compressive offset strain of 10% was applied and allowed to equilibrate before prescribing a sinusoidal shear strain profile, $\gamma = \gamma_0 \sin(\omega t)$ at an amplitude γ_o of 0.05 and an increasing angular frequency, ω, from 1 to 50 rad/s. The magnitude of the complex shear modulus was then calculated from $|G^*| = \tau_o/\gamma_o$, based on the assumption of linear, viscoelastic behavior, where the complex modulus, G^*, is obtained from the storage (G') and loss moduli (G'') as $G^* = G' + i\,G''$.

Tensile testing

Tensile experiments were performed on the scaffolds in a uniaxial configuration as previously described for cartilage[51,53] using an ELF 3200 materials testing system (SmartTest Series; Bose). Samples were cut into dumbbell-shaped coupons 25 mm in length and preloaded to 5 N. After equilibration of the preload, samples were elongated to failure at a rate of 0.04 mm/s. The resulting force was recorded by the instrument and divided by the cross-sectional area (A) of the sample at failure for calculation of the ultimate tensile stress ($\sigma = F/A$). Sequential images were recorded during testing using an automated digital video camera (Model XDC-X700; Sony Electronics, Park Ridge, NJ) and used to measure local strain.

Friction testing

Frictional tests were performed as described previously for cartilage[54] using the ARES Rheometrics System (Rheometric Scientific). The prescribed test was used to determine the dependence of the equilibrium friction coefficient, μ_{eq}, on angular velocity. Samples were fixed to an impermeable bottom platen using cyanoacrylate glue and immersed in a PBS bath. Before beginning the test, a compressive tare strain of 5% was applied to the sample using a stainless steel top platen and held for 1800 s, giving the imparted

stress time to relax to an equilibrium level. A series of sequential angular velocities, $\omega = 0.01$, 0.1, 1, and 10 rad/s, were subsequently applied through the bottom platen for a duration of 120 s each. During each step, normal force, N, and frictional torque, T, were recorded and used for calculation of equilibrium friction coefficient given by $\mu_{eq} = F/N$. By assuming that the distribution of unknown frictional shear is zero at the center and varies linearly along the radial direction of the cylindrical test specimen, the average frictional force, F, is given by $F = 4T/3r_0$, where r_0 is the radius of the specimen.

Histology and immunohistochemistry

Constructs from each experimental and control group was fixed in a 10% formalin buffered solution overnight at 4°C. After fixation, the constructs were dehydrated in graded ethanol solutions, cleared in xylene for a total of 3 h to dissolve away the PCL scaffold, embedded in paraffin wax, cut into 10-μm-thick cross sections using a Reichart–Jung microtome, and mounted on SuperFrost microscope slides (Microm International AG, Volketswil, Switzerland). The presence of collagen and sulfated glycosaminoglycans was histologically determined by treating 10 μm sections with hematoxylin for 3 min, 0.02% fast green for 3 min, and 0.1% aqueous safranin-O solution for 3 min. The sections were then rinsed in dH_2O and cleared in xylene. Human osteochondral tissue was used as a positive control. Immunohistochemical analysis was also performed on 10 μm sections. Pepsin digestion of the sections to be labeled for types I and II collagen was performed using Digest-All (Zymed, South San Francisco, CA), whereas those sections to be stained for chondroitin 4-sulfate were digested with trypsin, followed by a soybean trypsin inhibitor, and finally with chondroitinase (all from Sigma). Monoclonal antibodies were used to identify type I collagen (ab6308; Abcam, Cambridge, MA), type II collagen (II-II6B3; Developmental Studies Hybridoma Bank, University of Iowa, Iowa City, IA), and chondroitin 4-sulfate (2B6; gift from Dr. Virginia Kraus, Duke University Medical Center). Reagent A from the Histostain-Plus ES kit (Zymed) was used on all sections for serum blocking before primary and secondary antibody labeling (anti-mouse IgG antibody; Sigma Catalog No. B7151), whereas subsequent linkage to horseradish peroxidase was accomplished using Reagent C. The enzyme substrate–chromagen used for staining was aminoethyl carbazole (Zymed). Human osteochondral tissue was used as a positive control for type II collagen and chondroitin 4-sulfate antibodies, and the cartilage region was inspected to ensure antibody specificity. For the type I collagen antibody, human ligament was used as a positive control. Negative controls for each slide were also prepared to rule out nonspecific labeling, which was achieved by using blocking serum on the section versus the primary antibody during the primary antibody incubation step.

Statistical analysis

Two-factor analysis of variance with Fisher's protected least significant different (PLSD) *post hoc* test was performed to compare the different construct parameters (acellular vs. cellular and 3D PCL vs. 3D PCL–fibrin) for compressive, shear, and frictional biomechanical tests at each time point ($\alpha = 0.05$).

Results

Compression testing

At day 0, acellular 3D PCL scaffolds displayed an aggregate modulus (H_A) of 0.46 ± 0.04 MPa and a Young's modulus (E) of 0.27 ± 0.01 MPa, whereas acellular 3D PCL–fibrin composite scaffolds displayed an initial aggregate modulus of 0.67 ± 0.05 MPa and a Young's modulus of 0.74 ± 0.09 MPa (Fig. 2).

The initial compressive properties were maintained throughout the entire culture period, as no changes were observed for the scaffold type at either day 14 or day 28 (Fig. 3). Three-dimensioal PCL–fibrin composite scaffolds displayed significantly higher compressive moduli than 3D PCL scaffolds at all time points (H_A, $p < 0.005$; E, $p < 0.0001$). No significant differences in compressive moduli were observed between cellular and acellular groups; however, by day 28 an upward trend in stiffness was exhibited by the cell-loaded 3D PCL group versus its acellular control (Fig. 3A, B). This effect was not present in the 3D PCL–fibrin composite groups. Hydraulic permeability (k) of the acellular 3D PCL scaffolds at both days 14 and 28 was three orders of magnitude higher than all other groups tested (Fig. 3C, $p < 0.0001$).

Shear testing

The complex shear modulus (G^*) of both acellular scaffold types remained unchanged over culture time (Fig. 4A). However, cell-loaded 3D PCL constructs were 121% stiffer than acellular controls by day 14 and 315% stiffer than acellular controls by day 28. Likewise, cellular composite

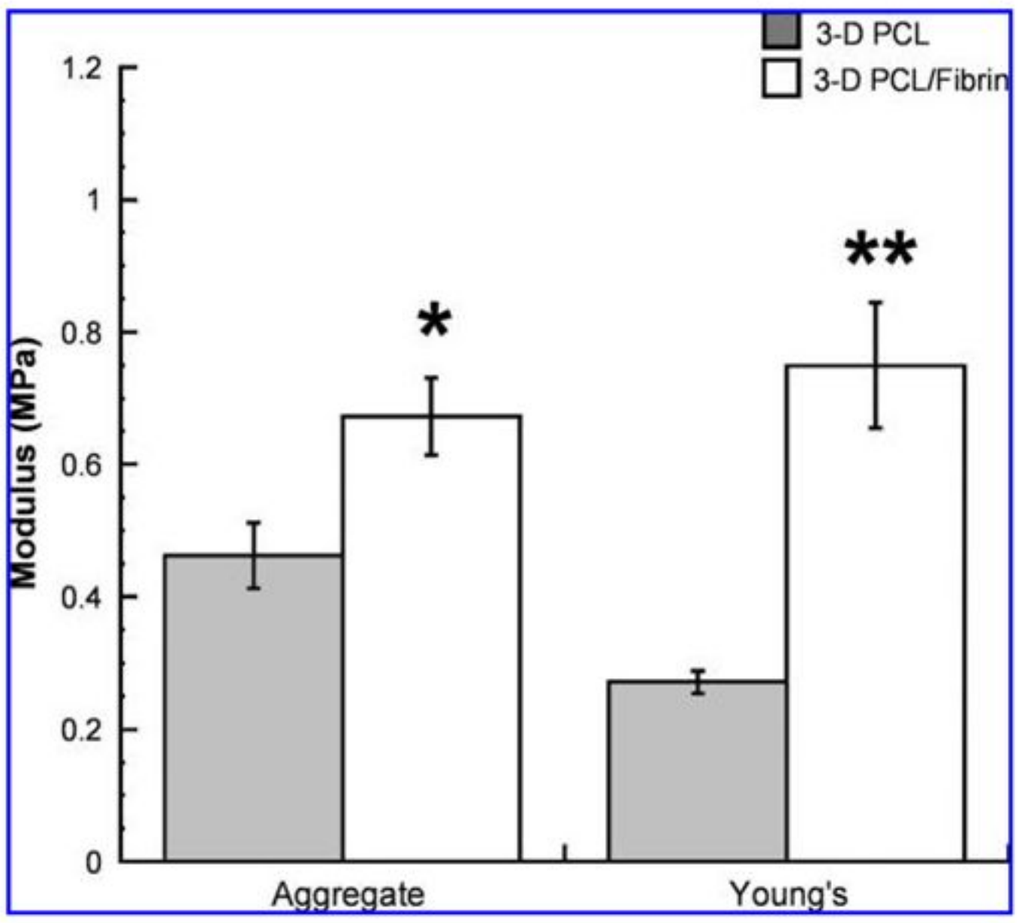

FIG. 2. The compressive stiffness of three-dimensional (3D) PCL scaffolds was increased when consolidated with fibrin. Aggregate modulus (H_A) and Young's modulus (E) at day 0 as determined by confined and unconfined compression, respectively. The 3D PCL–fibrin composite scaffolds had significantly higher H_A and E values than did naked 3D PCL scaffolds (analysis of variance [ANOVA], $^*p < 0.05$, $^{**}p < 0.0001$). Data presented as mean ± SEM.

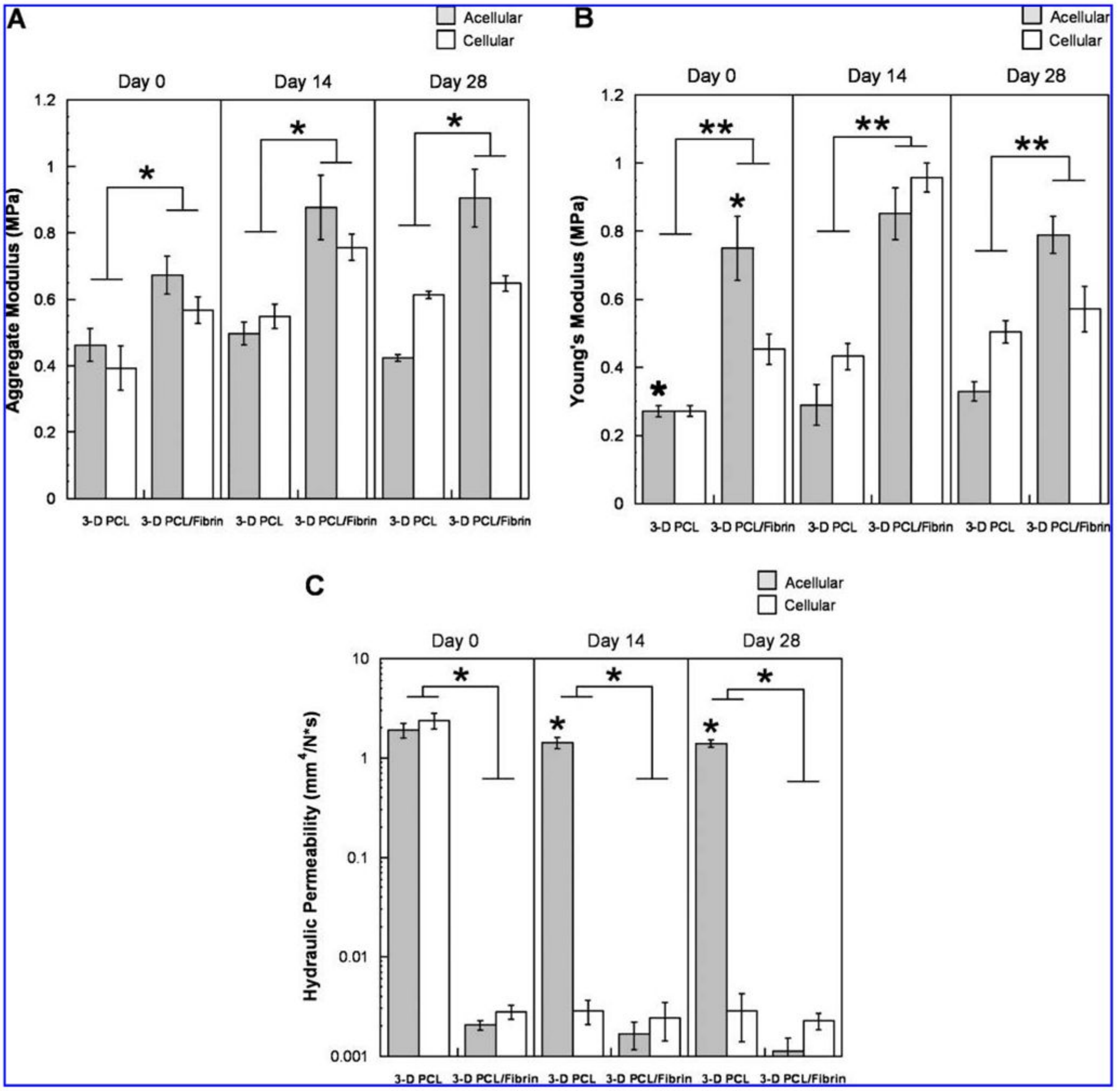

FIG. 3. Compressive biomechanical properties of scaffolds at days 0, 14, and 28. (**A**) Aggregate modulus (H_A) and (**B**) Young's modulus (E) as determined by confined and unconfined compression, respectively. The addition of fibrin to 3D PCL scaffolds significantly increased H_A and E for both cellular and acellular groups (ANOVA, $^*p < 0.05$, $^{**}p < 0.0001$). (**C**) Hydraulic permeability (k) as determined by curve-fitting creep tests using a numerical least-squares regression procedure. Acellular 3D PCL scaffolds displayed significantly higher k-values than all other groups at days 14 and 28 (ANOVA, $^*p < 0.0001$). Data represented as mean ± SEM.

constructs were 14% stiffer than acellular controls at day 14 and 12% stiffer than acellular controls at day 28 (Fig. 4A, $p < 0.001$). Similar to their behavior in compression, 3D PCL–fibrin scaffolds were significantly stiffer in shear compared with 3D PCL scaffolds (Fig. 4A). Acellular scaffolds displayed a greater loss angle (δ) compared with cell-loaded constructs at days 14 and 28 (Fig. 4B, $p < 0.005$). The values for loss angle fell between 20° and 30° for all groups, indicating viscoelastic solid-like behavior.

Tensile testing

At baseline, significant in-plane (x–y plane) anisotropy was observed in the ultimate tensile stress and tensile modulus measured at 10% strain. When tested in the x-direction, the ultimate tensile stress was 35.32 ± 1.90 MPa and the tensile modulus was 76.78 ± 8.11 MPa. When tested in the y-direction, the ultimate tensile stress was 22.90 ± 0.43 MPa ($p < 0.0001$) and the tensile modulus was 56.08 ± 5.51 MPa ($p = 0.0022$).

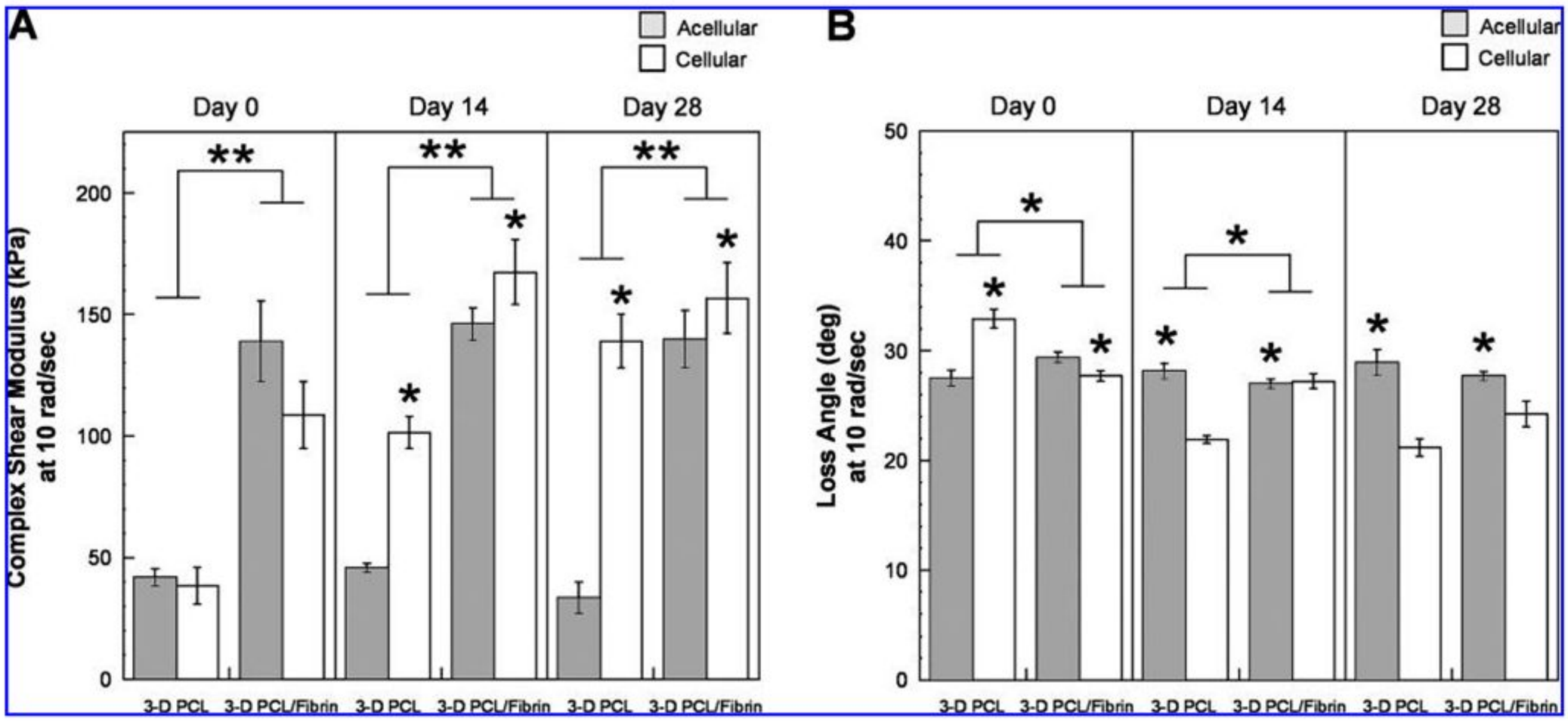

FIG. 4. Shear biomechanical properties of cultured scaffolds at days 14 and 28. (**A**) Complex shear modulus (G^*) and (**B**) loss angle (δ) measured at $\omega = 10\,\text{rad/s}$ and $\gamma_o = 0.05$. Adipose-derived stem cell–synthesized extracellular matrix significantly increased the shear stiffness of both 3D PCL and 3D PCL–fibrin composite scaffolds (ANOVA, $^*p < 0.05$, $^{**}p < 0.0001$). Data represented as mean ± SEM.

Friction testing

Acellular scaffolds exhibited similar equilibrium friction coefficients throughout the 28-day culture period (Fig. 5). Consolidating the 3D PCL scaffolds with fibrin resulted in an increase in baseline coefficients of friction measured at day 0. Cellular constructs displayed significantly higher coefficients of friction compared with acellular controls at days 14 and 28, with composite constructs appearing the highest (Fig. 5, $p < 0.001$). Porcine articular cartilage, tested as a control, exhibited a coefficient of friction of $\mu_{eq} = 0.27 \pm 0.04$.

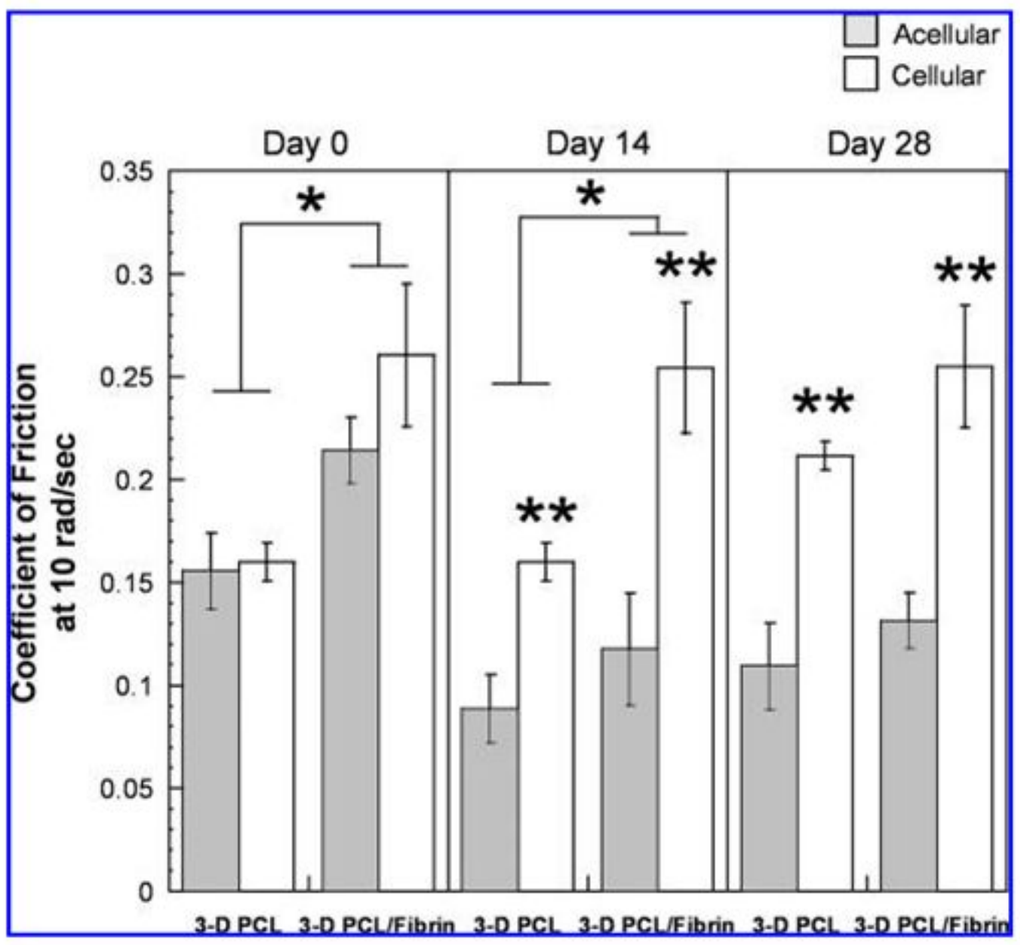

FIG. 5. Equilibrium coefficient of friction measured under steady frictional shear. Cellular constructs displayed significantly higher coefficients of friction against a rotating stainless steel platen than did acellular scaffolds (ANOVA, $^*p < 0.05$, $^{**}p < 0.001$). Data represented as mean ± SEM.

Histology and immunohistochemistry

Over time, ASC-synthesized tissue accumulated along the outer surfaces and within the internal pores of all cell-seeded constructs. Cells appeared evenly distributed with an elongated, fibroblast-like phenotype. Composite 3D PCL–fibrin constructs appeared to generate greater amounts of tissue than did 3D PCL constructs, as evidenced by stronger staining around the perimeter and throughout the thickness of these constructs. Histological analysis of both scaffold types revealed a highly cellular and fibrous matrix that stained strongly for collagen content, but exhibited low levels of safranin-O staining (Fig. 6). Immunostaining revealed the presence of the chondroitin 4-sulfate epitope, as well as types I and II collagen in both scaffold types. As seen with histology, staining appeared most intense around the perimeter of both scaffold types, with composite constructs showing stronger staining throughout their central region (Fig. 7).

Discussion

We have previously described the development and characterization of 3D woven composite scaffolds engineered with predetermined properties that reproduce the anisotropy, viscoelasticity, and tension–compression nonlinearity of native articular cartilage.[21] However, earlier studies revealed that after only 14 days of *in vitro* culture, the initial properties of these PGA-based constructs had sharply decreased as a result of rapid fiber degradation and a lack of functional ECM production from the embedded chondrocytes. The current study demonstrates that

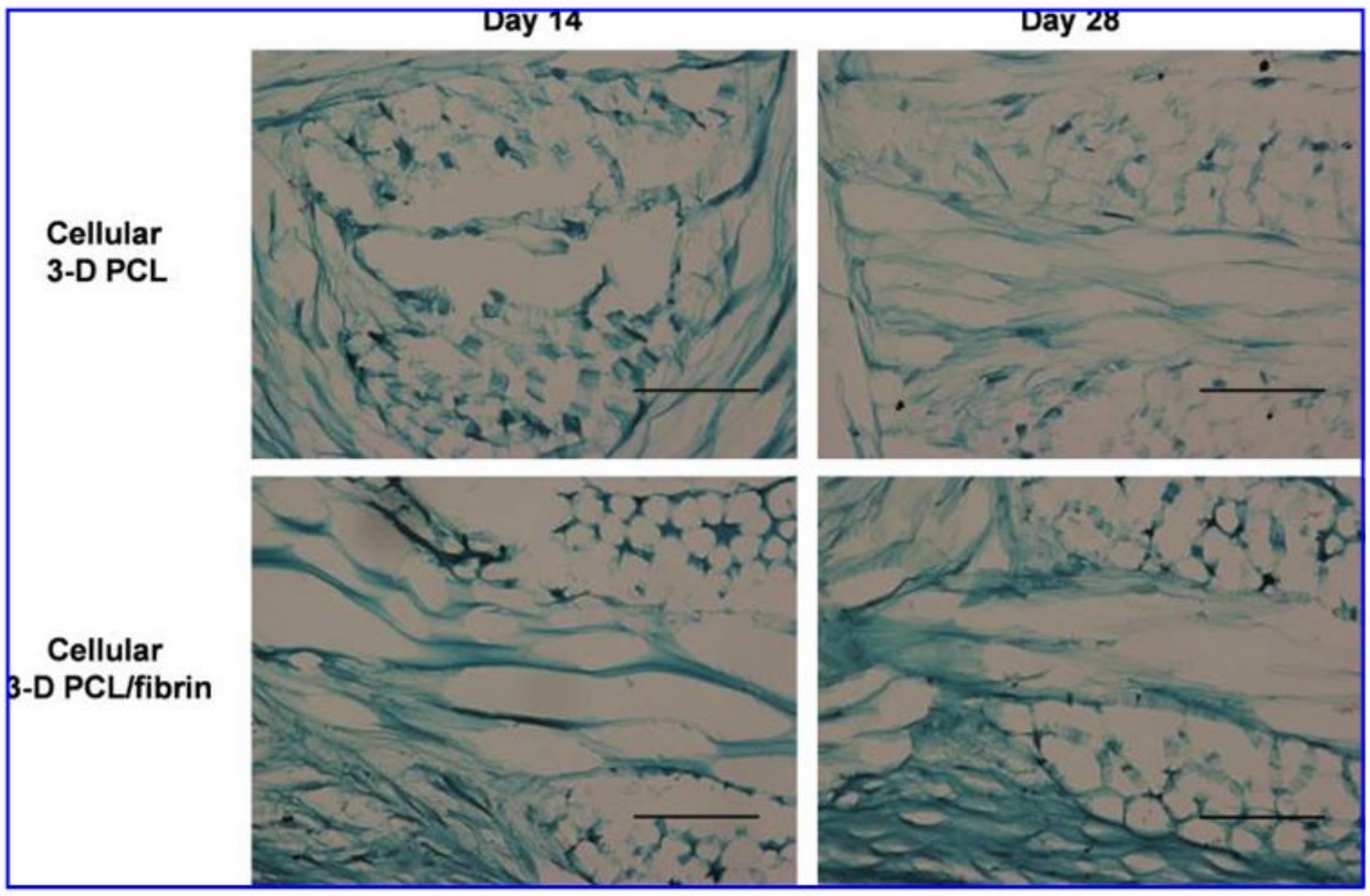

FIG. 6. Histology of cellular 3D PCL constructs and cellular 3D PCL–fibrin composite constructs at days 14 and 28 depicts fibrocartilaginous tissue synthesis within the 3D PCL scaffold. Scale bar = 100 μm. Color images available online at www.liebertonline.com/ten.

by replacing the PGA yarns of the woven scaffold with PCL yarns, structural properties never fell below their day 0 baseline values over a 28-day culture period. This behavior would allow an engineered construct to sustain its load-bearing properties over a sufficiently long period, during which functional new tissue could be regenerated. Further, by preserving the original 3D architecture and fiber–hydrogel composite construction, the PCL-based scaffolds used in this study retained the same anisotropy, viscoelasticity, and tension–compression nonlinearity displayed by the PGA-based scaffolds in our earlier work.[21] It should be emphasized that this scaffold structure was selected for use based on its ability to mimic the functional mechanical properties of articular cartilage. Although the reinforcing yarns of the scaffold provide directionally dependent load support similar to the collagen ultrastructure of native cartilage, their scale and organization throughout the tissue differ significantly. As such, the engineered constructs in this study demonstrated a distinct structure compared with normal cartilage histology (Figs. 6 and 7), while retaining the mechanical properties critical to normal tissue function.

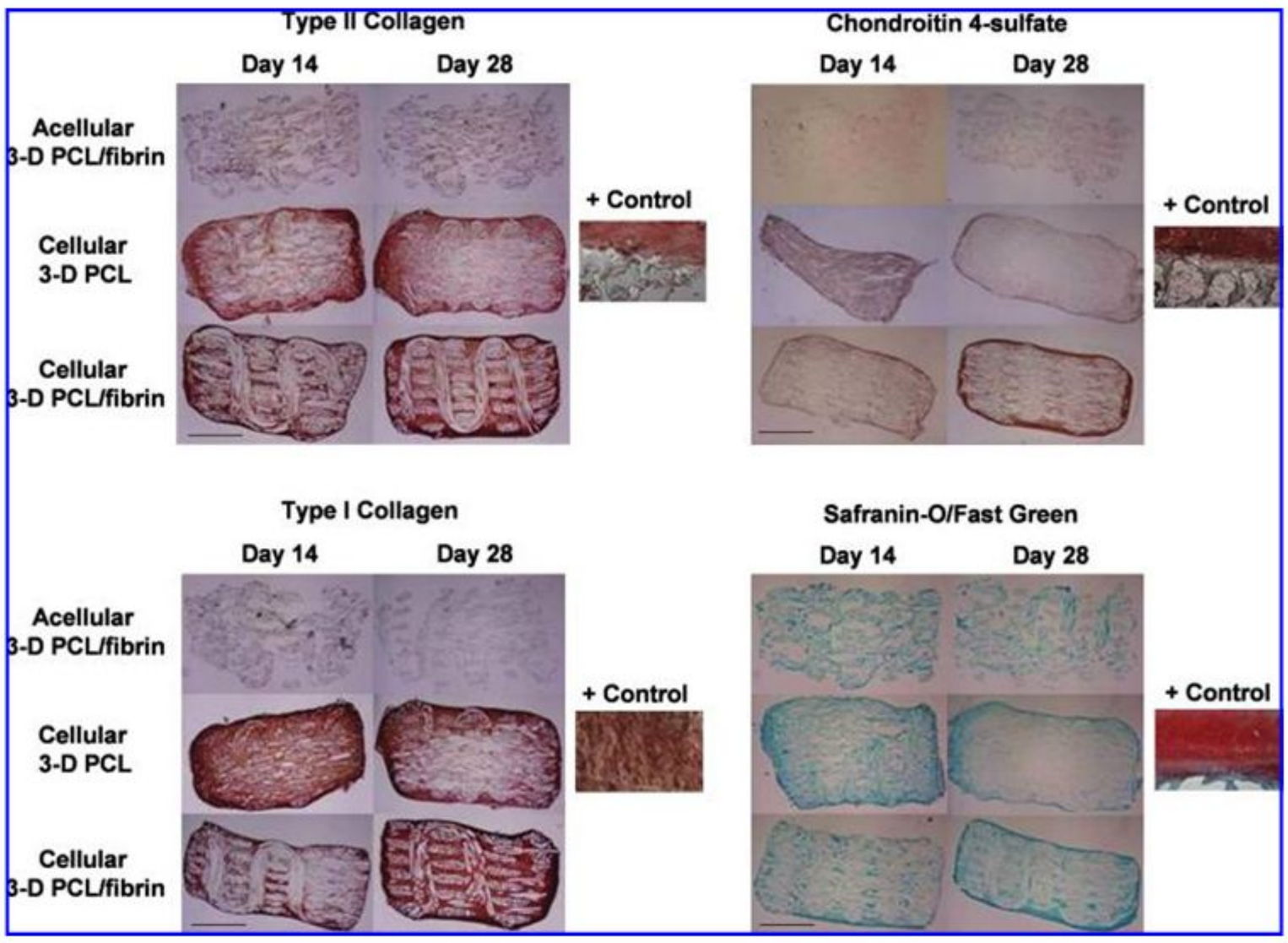

FIG. 7. Histology and immunohistochemistry of acellular 3D PCL–fibrin composite scaffolds, cellular 3D PCL constructs, and cellular 3D PCL–fibrin composite constructs at days 14 and 28. Scale bar = 1 mm. Color images available online at www.liebertonline.com/ten.

Confined compression testing performed in this study revealed that the initial (day 0) aggregate modulus of the acellular 3D PCL scaffold was increased 70% by consolidating it with fibrin to form a composite (Fig. 2). In compression, the 3D woven structure resists deformation due to inter- and intrafiber friction between its constituent multifilament yarns. However, under compression, these yarn bundles can slip relative to one another and distort their cross-sectional shape. When formed into a composite, the fibrin matrix acts to bind and constrain the yarns within their woven conformation, limiting relative movement and effectively stiffening the structure. This effect was even more pronounced when testing in the unconfined configuration where scaffolds are not laterally constrained, as Young's modulus of the 3D PCL–fibrin composite was 270% higher than that of the naked 3D PCL. Compression tests performed at days 14 and 28 revealed that all acellular scaffolds maintained their initial properties throughout the culture period, indicating that no mechanically significant degradation had occurred to either the PCL fibers or the fibrin hydrogel (Fig. 3A, B). For cell-loaded constructs, the newly synthesized tissue had no significant effect on aggregate or Young's moduli. However, the cellular 3D PCL group demonstrated an increasing trend in these properties over time, which likely resulted from the ECM acting to constrain the woven structure as the fibrin matrix did in the acellular scaffolds. Interestingly, by day 28 the cellular 3D PCL–fibrin constructs appeared to have lower compressive moduli than the acellular 3D PCL–fibrin scaffolds. This reduction in properties may reflect cell-mediated degradation of the fibrin at a rate that exceeds new tissue synthesis. Alternatively, these findings may be attributed to increased accumulation of neotissue along the outer surfaces of the woven scaffold, which acts to form a deformable layer that effectively reduces the apparent stiffness of the structure (Fig. 6). The apparent hydraulic permeability of the porous 3D scaffolds, as measured by confined compression creep, declined by three orders of magnitude when consolidated with fibrin (in acellular 3D PCL–fibrin groups), ECM (in cellular 3D PCL groups), or a combination of the two (in cellular 3D PCL–fibrin groups) (Fig. 3C). In these cases, the large interconnected pores of the woven structure were completely filled with a less permeable matrix material, resulting in values that compared well to those of native cartilage ($k = 0.0005$–$0.005\,\mathrm{mm}^4/\mathrm{N}\cdot\mathrm{s}$).[55,56]

As with the compressive properties (H_A, E, and k) evaluated in this study, the shear properties (G^* and δ) of the acellular scaffolds were improved by consolidating the 3D PCL with fibrin gel (Fig. 4A, B). These properties were also maintained over the entire culture period, further suggesting that no constituent material degradation had occurred. The 3D orthogonal structure used in this study has an inherently low resistance to shear deformation due to a lack of interlacing between the stacked fiber layers that build its thickness (Fig. 1). In the current study, we tested a scaffold consisting of 11 layers with an overall thickness of 1.4 mm, although in practicality, a wide range of thicknesses could be constructed depending on the fiber diameter, number of layers, and other weaving parameters. As a result, the ASC-synthesized ECM in the cellular constructs had a greater effect on shear properties than on compressive properties, as evidenced by the significant increase in complex shear modulus at days 14 and 28. This matrix-stiffening effect was greatest for the 3D PCL group (121% increase at day 14 and 315% increase at day 28), where new ECM gradually fills the empty pores of the scaffold and binds the structure. In the 3D PCL–fibrin group, the scaffold stiffness was significantly increased by the consolidating fibrin matrix before culture; therefore, the accumulation of new ECM had a lesser (14% increase at day 14 and 12% increase at day 28) effect overall on the scaffold structure due to its composite construction. Further, the lower loss angles measured for cell-loaded constructs further indicated that the accumulated neotissue stiffened the scaffolds and improved their biomechanical properties.

Although the tensile properties of the constructs were not measured over time in culture due to the limited size of the specimens, baseline properties compared well to those of native cartilage, reported in the literature as 15–35 MPa for ultimate tensile stress[57,58] and 5–25.5 MPa for tensile modulus at 10% strain.[51,59] Similar to articular cartilage, PCL scaffolds displayed a difference in tensile and compressive stiffness of approximately two orders of magnitude. This tension–compression nonlinearity is believed to play a crucial role in the load-bearing and lubrication properties of the native tissue.[60,61]

A novel and important finding of this study was that 3D woven scaffold exhibited an equilibrium coefficient of friction similar to that of native articular cartilage, that is, $\mu_{eq} \sim 0.1$–0.3. These findings are in general agreement with previous studies that have measured the frictional properties of engineered cartilage constructs.[62–66] In these previous studies, it has been shown that a number of factors such as the scaffold, culture conditions, and cell type may influence the equilibrium frictional properties over time in culture. In several cases, however, it has been shown that engineered constructs may exhibit a similar or even lower μ_{eq} than native cartilage, as was observed in the present study.[62,63] A consideration in the interpretation of this work is that we did not measure the dynamic, early-time coefficient of friction, which is generally believed to depend on fluid load support and can be 1–2 orders of magnitude lower than μ_{eq}[54,61] and is dependent on the tensile properties of tissue in the transverse direction to loading.[67] In this respect, the high tension–compression nonlinearity and low hydraulic permeability of the 3D woven constructs would be expected to provide fluid pressurization and load support that would reduce the short-term frictional properties. Ultimately, however, while frictional properties provide an important measure of the functional behavior of the cartilage, the wear properties may reflect a more relevant measure of the long-term durability of the construct, and additional studies will be needed to measure the dynamic friction and wear behavior of engineered cartilage constructs.

The fibrin gel used in this composite scaffold system served a dual purpose in influencing the bulk construct properties by stiffening and consolidating the woven structure and by enhancing the biological function of the scaffold by providing a natural ECM that interacts with ASCs.[33] The Tisseel fibrin sealant used in this study was selected due to its known chemoattractive properties that promote the migration and proliferation of human chondrocytes.[68,69] As determined by histological and immunohistochemical analyses, ASCs seeded on 3D PCL–fibrin composites appeared to produce

greater amounts of collagen-rich ECM, on both the outer surfaces and within the inner pores, than did ASCs seeded on 3D PCL alone. However, it should be noted that, overall, these constructs demonstrated a fibrocartilaginous phenotype, as safranin-O staining for proteoglycans was low and both type I collagen and type II collagen were synthesized.

Conclusions

The findings of this study show that 3D fiber-reinforced composite scaffolds, which are designed to mimic the biomechanical behavior of native articular cartilage, can sustain their initial properties over an extended *in vitro* cultivation period by the selection of appropriate constituent materials. Specifically, the use of slowly degrading PCL gives the constructs evaluated in this study long-term stability, maintaining a biomechanically functional framework that affords seeded cells ample time to synthesize a new ECM. Despite a fibrocartilaginous phenotype, constructs exhibited relatively constant mechanical properties over a 28-day culture period, with aggregate, Young's, and complex shear moduli similar to those of native cartilage. Histological and immunohistochemical analyses of ASC-seeded constructs revealed a contiguous, collagen-rich ECM that encapsulated the outer surfaces of the scaffolds, while completely filling their internal pores. One characteristic of this study was that exogenous growth factors were not used to induce chondrogenesis of the ASCs, to examine the ability of the scaffold itself to induce tissue formation. Future experiments incorporating potent factors such as BMP-6 and TGF-β[30,31] may facilitate more cartilage-like tissue formation on the composite scaffolds and improve the overall biomechanical behavior of the engineered constructs.

Acknowledgments

Supported by NIH Grants AR50245, AG15768, AR55042, AR48182, and AR48852, the Wallace H. Coulter Foundation, and the Duke Translational Research Institute. We thank Dr. Bill Tawil and Elizabeth Hagerman of Baxter Biosurgery for providing Tisseel, Simon Sutter of EMS-Griltech for generously donating PCL fiber, Dr. Lisa Freed for many helpful discussions, and Melanie Kolkin and Jonathan Brunger for technical assistance.

Disclosure Statement

One of the authors (FG) owns equity in Cytex Therapeutics, Inc. The other author has no competing financial interests.

References

1. Hunziker, E.B. Articular cartilage repair: basic science and clinical progress. A review of the current status and prospects. Osteoarthritis Cartilage **10,** 432, 2002.
2. Chu, C.R., Convery, F.R., Akeson, W.H., Meyers, M., and Amiel, D. Articular cartilage transplantation. Clinical results in the knee. Clin Orthop Relat Res **360,** 159, 1999.
3. Minas, T., and Nehrer, S. Current concepts in the treatment of articular cartilage defects. Orthopedics **20,** 525, 1997.
4. Shapiro, F., Koide, S., and Glimcher, M.J. Cell origin and differentiation in the repair of full-thickness defects of articular cartilage. J Bone Joint Surg Am **75,** 532, 1993.
5. Smith, G.D., Knutsen, G., and Richardson, J.B. A clinical review of cartilage repair techniques. J Bone Joint Surg Br **87,** 445, 2005.
6. Guilak, F., Butler, D.L., and Goldstein, S.A. Functional tissue engineering: the role of biomechanics in articular cartilage repair. Clin Orthop Relat Res **391 Suppl,** S295, 2001.
7. Butler, D.L., Goldstein, S.A., and Guilak, F. Functional tissue engineering: the role of biomechanics. J Biomech Eng **122,** 570, 2000.
8. Boublik, J., Park, H., Radisic, M., Tognana, E., Chen, F., Pei, M., Vunjak-Novakovic, G., and Freed, L.E. Mechanical properties and remodeling of hybrid cardiac constructs made from heart cells, fibrin, and biodegradable, elastomeric knitted fabric. Tissue Eng **11,** 1122, 2005.
9. Dong, H., Ye, J.D., Wang, X.P., and Yang, J.J. Preparation of calcium phosphate cement tissue engineering scaffold reinforced with chitin fiber. J Inorg Mater **22,** 1007, 2007.
10. Guarino, V., and Ambrosio, L. The synergic effect of polylactide fiber and calcium phosphate particle reinforcement in poly epsilon-caprolactone-based composite scaffolds. Acta Biomater **4,** 1778, 2008.
11. Thomson, R.C., Yaszemski, M.J., Powers, J.M., and Mikos, A.G. Hydroxyapatite fiber reinforced poly(alpha-hydroxy ester) foams for bone regeneration. Biomaterials **19,** 1935, 1998.
12. Altman, G.H., Horan, R.L., Lu, H.H., Moreau, J., Martin, I., Richmond, J.C., and Kaplan, D.L. Silk matrix for tissue engineered anterior cruciate ligaments. Biomaterials **23,** 4131, 2002.
13. Horan, R.L., Collette, A.L., Lee, C., Antle, K., Chen, J.S., and Altman, G.H. Yarn design for functional tissue engineering. J Biomech **39,** 2232, 2006.
14. Laurencin, C.T., and Freeman, J.W. Ligament tissue engineering: an evolutionary materials science approach. Biomaterials **26,** 7530, 2005.
15. Baker, B.M., and Mauck, R.L. The effect of nanofiber alignment on the maturation of engineered meniscus constructs. Biomaterials **28,** 1967, 2007.
16. Li, W.J., Cooper, J.A., Mauck, R.L., and Tuan, R.S. Fabrication and characterization of six electrospun poly(alpha-hydroxy ester)-based fibrous scaffolds for tissue engineering applications. Acta Biomater **2,** 377, 2006.
17. Chen, G., Sato, T., Ushida, T., Hirochika, R., Shirasaki, Y., Ochiai, N., and Tateishi, T. The use of a novel PLGA fiber/collagen composite web as a scaffold for engineering of articular cartilage tissue with adjustable thickness. J Biomed Mater Res A **67,** 1170, 2003.
18. Schmal, H., Mehlhorn, A.T., Kurze, C., Zwingmann, J., Niemeyer, P., Finkenzeller, G., Dauner, M., Sudkamp, N.P., and Kostler, W. [*In vitro* study on the influence of fibrin in cartilage constructs based on PGA fleece materials]. Orthopade **37,** 424, 2008.
19. Slivka, M.A., Leatherbury, N.C., Kieswetter, K., and Niederauer, G.G. Porous, resorbable, fiber-reinforced scaffolds tailored for articular cartilage repair. Tissue Eng **7,** 767, 2001.
20. Webb, A.R., Macrie, B.D., Ray, A.S., Russo, J.E., Siegel, A.M., Glucksberg, M.R., and Ameer, G.A. *In vitro* characterization of a compliant biodegradable scaffold with a novel bioreactor system. Ann Biomed Eng **35,** 1357, 2007.
21. Moutos, F.T., Freed, L.E., and Guilak, F. A biomimetic three-dimensional woven composite scaffold for functional tissue engineering of cartilage. Nat Mater **6,** 162, 2007.
22. Moutos, F.T., and Guilak, F. Composite scaffolds for cartilage tissue engineering. Biorheology **45,** 501, 2008.

23. Moutos, F.T. Biomimetic composite scaffolds for the functional tissue engineering of articular cartilage. Doctoral dissertation, Duke University, Durham, NC, 2009.
24. Knutsen, G., Engebretsen, L., Ludvigsen, T.C., Drogset, J.O., Grontvedt, T., Solheim, E., Strand, T., Roberts, S., Isaksen, V., and Johansen, O. Autologous chondrocyte implantation compared with microfracture in the knee. A randomized trial. J Bone Joint Surg Am **86A,** 455, 2004.
25. Lee, C.R., Grodzinsky, A.J., Hsu, H.P., Martin, S.D., and Spector, M. Effects of harvest and selected cartilage repair procedures on the physical and biochemical properties of articular cartilage in the canine knee. J Orthop Res **18,** 790, 2000.
26. Stokes, D.G., Liu, G., Coimbra, I.B., Piera-Velazquez, S., Crowl, R.M., and Jimenez, S.A. Assessment of the gene expression profile of differentiated and dedifferentiated human fetal chondrocytes by microarray analysis. Arthritis Rheum **46,** 404, 2002.
27. Thirion, S., and Berenbaum, F. Culture and phenotyping of chondrocytes in primary culture. Methods Mol Med **100,** 1, 2004.
28. Erickson, G.R., Gimble, J.M., Franklin, D.M., Rice, H.E., Awad, H., and Guilak, F. Chondrogenic potential of adipose tissue-derived stromal cells *in vitro* and *in vivo*. Biochem Biophys Res Commun **290,** 763, 2002.
29. Wei, Y.Y., Hu, Y., Hao, W., Han, Y.S., Meng, G.L., Zhang, D.Z., Wu, Z.X., and Wang, H.Q. A novel injectable scaffold for cartilage tissue engineering using adipose-derived adult stem cells. Journal of Orthopaedic Research **26,** 27, 2008.
30. Estes, B.T., Wu, A.W., and Guilak, F. Potent induction of chondrocytic differentiation of human adipose-derived adult stem cells by bone morphogenetic protein 6. Arthritis Rheum **54,** 1222, 2006.
31. Hennig, T., Lorenz, H., Thiel, A., Goetzke, K., Dickhut, A., Geiger, F., and Richter, W. Reduced chondrogenic potential of adipose tissue derived stromal cells correlates with an altered TGF beta receptor and BMP profile and is overcome by BMP-6. J Cell Physiol **211,** 682, 2007.
32. Sheyn, D., Pelled, G., Zilberman, Y., Talasazan, F., Frank, J.M., Gazit, D., and Gazit, Z. Nonvirally engineered porcine adipose tissue-derived stem cells: use in posterior spinal fusion. Stem Cells **26,** 1056, 2008.
33. Awad, H.A., Wickham, M.Q., Leddy, H.A., Gimble, J.M., and Guilak, F. Chondrogenic differentiation of adipose-derived adult stem cells in agarose, alginate, and gelatin scaffolds. Biomaterials **25,** 3211, 2004.
34. Eyrich, D., Brandl, F., Appel, B., Wiese, H., Maier, G., Wenzel, M., Staudenmaier, R., Goepferich, A., and Blunk, T. Long-term stable fibrin gels for cartilage engineering. Biomaterials **28,** 55, 2007.
35. Passaretti, D., Silverman, R.P., Huang, W., Kirchhoff, C.H., Ashiku, S., Randolph, M.A., and Yaremchuk, M.J. Cultured chondrocytes produce injectable tissue-engineered cartilage in hydrogel polymer. Tissue Eng **7,** 805, 2001.
36. Peretti, G.M., Randolph, M.A., Zaporojan, V., Bonassar, L.J., Xu, J.W., Fellers, J.C., and Yaremchuk, M.J. A biomechanical analysis of an engineered cell-scaffold implant for cartilage repair. Ann Plast Surg **46,** 533, 2001.
37. Silverman, R.P., Passaretti, D., Huang, W., Randolph, M.A., and Yaremchuk, M. Injectable tissue-engineered cartilage using a fibrin glue polymer. Plast Reconstr Surg **103,** 1809, 1999.
38. Xu, J.W., Zaporojan, V., Peretti, G.M., Roses, R.E., Morse, K.B., Roy, A.K., Mesa, J.M., Randolph, M.A., Bonassar, L.J., and Yaremchuk, M.J. Injectable tissue-engineered cartilage with different chondrocyte sources. Plast Reconstr Surg **113,** 1361, 2004.
39. Weinand, C., Gupta, R., Huang, A.Y., Weinberg, E., Madisch, I., Qudsi, R.A., Neville, C.M., Pomerantseva, I., and Vacanti, J.P. Comparison of hydrogels in the *in vivo* formation of tissue-engineered bone using mesenchymal stem cells and beta-tricalcium phosphate. Tissue Eng **13,** 757, 2007.
40. Xu, J.W., Nazzal, J., Peretti, G.M., Kirchhoff, C.H., Randolph, M.A., and Yaremchuk, M.J. Tissue-engineered cartilage composite with expanded polytetrafluoroethylene membrane. Ann Plast Surg **46,** 527, 2001.
41. Van Lieshout, M., Peters, G., Rutten, M., and Baaijens, F. A knitted, fibrin-covered polycaprolactone scaffold for tissue engineering of the aortic valve. Tissue Eng **12,** 481, 2006.
42. Huang, M.H., Li, S.M., Hutmacher, D.W., Coudane, J., and Vert, M. Degradation characteristics of poly(epsilon-caprolactone)-based copolymers and blends. J Appl Polym Sci **102,** 1681, 2006.
43. Rohner, D., Hutmacher, D.W., Cheng, T.K., Oberholzer, M., and Hammer, B. *In vivo* efficacy of bone-marrow-coated polycaprolactone scaffolds for the reconstruction of orbital defects in the pig. J Biomed Mater Res B Appl Biomater **66,** 574, 2003.
44. Chew, S.Y., Wen, Y., Dzenis, Y., and Leong, K.W. The role of electrospinning in the emerging field of nanomedicine. Curr Pharm Des **12,** 4751, 2006.
45. Huang, Q., Goh, J.C., Hutmacher, D.W., and Lee, E.H. *In vivo* mesenchymal cell recruitment by a scaffold loaded with transforming growth factor beta1 and the potential for in situ chondrogenesis. Tissue Eng **8,** 469, 2002.
46. Hutmacher, D.W. Scaffold design and fabrication technologies for engineering tissues—state of the art and future perspectives. J Biomater Sci Polym Ed **12,** 107, 2001.
47. Zein, I., Hutmacher, D.W., Tan, K.C., and Teoh, S.H. Fused deposition modeling of novel scaffold architectures for tissue engineering applications. Biomaterials **23,** 1169, 2002.
48. Ng, K.W., Khor, H.L., and Hutmacher, D.W. *In vitro* characterization of natural and synthetic dermal matrices cultured with human dermal fibroblasts. Biomaterials **25,** 2807, 2004.
49. Serrano, M.C., Portoles, M.T., Vallet-Regi, M., Izquierdo, I., Galletti, L., Comas, J.V., and Pagani, R. Vascular endothelial and smooth muscle cell culture on NaOH-treated poly(epsilon-caprolactone) films: a preliminary study for vascular graft development. Macromol Biosci **5,** 415, 2005.
50. Tsuji, H., Ishida, T., and Fukuda, N. Surface hydrophilicity and enzymatic hydrolyzability of biodegradable polyesters: 1. Effects of alkaline treatment. Polym Int **52,** 843, 2003.
51. Elliott, D.M., Guilak, F., Vail, T.P., Wang, J.Y., and Setton, L.A. Tensile properties of articular cartilage are altered by meniscectomy in a canine model of osteoarthritis. J Orthop Res **17,** 503, 1999.
52. Mow, V.C., Kuei, S.C., Lai, W.M., and Armstrong, C.G. Biphasic creep and stress relaxation of articular cartilage in compression? Theory and experiments. J Biomech Eng **102,** 73, 1980.
53. Guilak, F., Ratcliffe, A., Lane, N., Rosenwasser, M.P., and Mow, V.C. Mechanical and biochemical changes in the superficial zone of articular cartilage in canine experimental osteoarthritis. J Orthop Res **12,** 474, 1994.
54. Wang, H., and Ateshian, G.A. The normal stress effect and equilibrium friction coefficient of articular cartilage under steady frictional shear. J Biomech **30,** 771, 1997.

55. Athanasiou, K.A., Rosenwasser, M.P., Buckwalter, J.A., Malinin, T.I., and Mow, V.C. Interspecies comparisons of in situ intrinsic mechanical properties of distal femoral cartilage. J Orthop Res **9,** 330, 1991.
56. Setton, L.A., Zhu, W., and Mow, V.C. The biphasic poroviscoelastic behavior of articular cartilage: role of the surface zone in governing the compressive behavior. J Biomech **26,** 581, 1993.
57. Bader, D.L., Kempson, G.E., Barrett, A.J., and Webb, W. The effects of leucocyte elastase on the mechanical properties of adult human articular cartilage in tension. Biochim Biophys Acta **677,** 103, 1981.
58. Kempson, G.E., Tuke, M.A., Dingle, J.T., Barrett, A.J., and Horsfield, P.H. The effects of proteolytic enzymes on the mechanical properties of adult human articular cartilage. Biochim Biophys Acta **428,** 741, 1976.
59. Akizuki, S., Mow, V.C., Muller, F., Pita, J.C., Howell, D.S., and Manicourt, D.H. Tensile properties of human knee joint cartilage: I. Influence of ionic conditions, weight bearing, and fibrillation on the tensile modulus. J Orthop Res **4,** 379, 1986.
60. Li, W.J., Jiang, Y.J., and Tuan, R.S. Chondrocyte phenotype in engineered fibrous matrix is regulated by fiber size. Tissue Eng **12,** 1775, 2006.
61. Soltz, M.A., and Ateshian, G.A. Experimental verification and theoretical prediction of cartilage interstitial fluid pressurization at an impermeable contact interface in confined compression. J Biomech **31,** 927, 1998.
62. Ando, W., Tateishi, K., Hart, D.A., Katakai, D., Tanaka, Y., Nakata, K., Hashimoto, J., Fujie, H., Shino, K., Yoshikawa, H., and Nakamura, N. Cartilage repair using an *in vitro* generated scaffold-free tissue-engineered construct derived from porcine synovial mesenchymal stem cells. Biomaterials **28,** 5462, 2007.
63. Gleghorn, J.P., Jones, A.R., Flannery, C.R., and Bonassar, L.J. Boundary mode frictional properties of engineered cartilaginous tissues. Eur Cell Mater **14,** 20; discussion 28, 2007.
64. Lima, E.G., Bang, L.M., Serebrov, A., Mauck, R., Byers, B.A., Tuan, R., Ateshian, G.A., and Hung, C.T. Measuring the frictional properties of tissue-engineered cartilage constructs. Trans Orthop Res Soc **31,** 1501, 2006.
65. Plainfosse, M., Hatton, P.V., Crawford, A., Jin, Z.M., and Fisher, J. Influence of the extracellular matrix on the frictional properties of tissue-engineered cartilage. Biochem Soc Trans **35(Pt 4),** 677, 2007.
66. Morita, Y., Tomita, N., Aoki, H., Sonobe, M., Wakitani, S., Tamada, Y., Suguro, T., and Ikeuchi, K. Frictional properties of regenerated cartilage *in vitro*. J Biomech **39,** 103, 2006.
67. Krishnan, R., Park, S., Eckstein, F., and Ateshian, G.A. Inhomogeneous cartilage properties enhance superficial interstitial fluid support and frictional properties, but do not provide a homogeneous state of stress. J Biomech Eng **125,** 569, 2003.
68. Kirilak, Y., Pavlos, N.J., Willers, C.R., Han, R., Feng, H., Xu, J., Asokananthan, N., Stewart, G.A., Henry, P., Wood, D., and Zheng, M.H. Fibrin sealant promotes migration and proliferation of human articular chondrocytes: possible involvement of thrombin and protease-activated receptors. Int J Mol Med **17,** 551, 2006.
69. Willers, C., Chen, J., Wood, D., Xu, J., and Zheng, M.H. Autologous chondrocyte implantation with collagen bioscaffold for the treatment of osteochondral defects in rabbits. Tissue Eng **11,** 1065, 2005.

Address correspondence to:
Farshid Guilak, Ph.D.
Department of Surgery
Duke University Medical Center
375 MSRB, Box 3093
Durham, NC 27710

E-mail: guilak@duke.edu

Received: July 14, 2009
Accepted: November 9, 2009
Online Publication Date: December 16, 2009

This article has been cited by:

1. Christoffer K. Abrahamsson , Fan Yang , Hyoungshin Park , Jonathan M. Brunger , Piia K. Valonen , Robert Langer , Jean F. Welter , Arnold I. Caplan , Farshid Guilak , Lisa E. Freed . 2010. Chondrogenesis and Mineralization During In Vitro Culture of Human Mesenchymal Stem Cells on Three-Dimensional Woven ScaffoldsChondrogenesis and Mineralization During In Vitro Culture of Human Mesenchymal Stem Cells on Three-Dimensional Woven Scaffolds. *Tissue Engineering Part A* **16**:12, 3709-3718. [Abstract] [Full Text] [PDF] [PDF Plus]
2. Claire G. Jeong , Scott J. Hollister . 2010. Mechanical and Biochemical Assessments of Three-Dimensional Poly(1,8-Octanediol-co-Citrate) Scaffold Pore Shape and Permeability Effects on In Vitro Chondrogenesis Using Primary ChondrocytesMechanical and Biochemical Assessments of Three-Dimensional Poly(1,8-Octanediol-co-Citrate) Scaffold Pore Shape and Permeability Effects on In Vitro Chondrogenesis Using Primary Chondrocytes. *Tissue Engineering Part A* **16**:12, 3759-3768. [Abstract] [Full Text] [PDF] [PDF Plus]
3. Franklin T. Moutos, Bradley T. Estes, Farshid Guilak. 2010. Multifunctional Hybrid Three-dimensionally Woven Scaffolds for Cartilage Tissue Engineering. *Macromolecular Bioscience* **10**:11, 1355-1364. [CrossRef]
4. Farshid Guilak, Bradley T. Estes, Brian O. Diekman, Franklin T. Moutos, Jeffrey M. Gimble. 2010. 2010 Nicolas Andry Award: Multipotent Adult Stem Cells from Adipose Tissue for Musculoskeletal Tissue Engineering. *Clinical Orthopaedics and Related Research®* **468**:9, 2530-2540. [CrossRef]
5. Seth D. McCullen, Carla M. Haslauer, Elizabeth G. Loboa. 2010. Fiber-reinforced scaffolds for tissue engineering and regenerative medicine: use of traditional textile substrates to nanofibrous arrays. *Journal of Materials Chemistry* **20**:40, 8776. [CrossRef]